Available online at www.sciencedirect.com

ScienceDirect

Energy Procedia 121 (2017) 118–125

Energy Procedia

www.elsevier.com/locate/procedia

International Conference on Improving Residential Energy Efficiency, IREE 2017

Thermal performance evaluation of an integrated photovoltaic thermal-phase change material system using Taguchi method

Haoshan Ren[a,]*, Wenye Lin[a], Zhenjun Ma[a], Wenke Fan[a]

[a]*Sustainable Buildings Research Centre (SBRC), University of Wollongong, Wollongong, NSW, 2522*

Abstract

This paper presents the performance evaluation of an integrated photovoltaic thermal (PVT) collector-phased change material (PCM) thermal energy storage (TES) system. The PVT collectors can generate both electricity and low-grade thermal energy during the daytime, and the thermal energy generated can be temporarily stored in the PCM TES unit and used for space heating during the night-time. Taguchi method and analysis of variance are used for the simulation design and data analysis, respectively. The thermal performance of the proposed system was evaluated in terms of the useful energy stored in the TES system. The results showed that the outlet air temperature of the TES unit remained at least 2°C higher than the inlet air temperature during the discharging process in the selected test day. The PCM type and the PCM charging air flow rate were the most important factors influencing the useful energy stored in the TES system.

Peer-review under responsibility of the scientific committee of the International Conference on Improving Residential Energy Efficiency.

Keywords: Photovoltaic thermal collector; Phase change material; Thermal energy storage; Domestic space heating.

1. Introduction

Buildings are one of the major energy consumers and account for around 40% of total energy use worldwide in 2015 [1]. In the building sector, a significant amount of energy was used by heating, ventilation, and air conditioning (HVAC) systems. In order to reduce the energy consumption of building HVAC systems, many

* Corresponding author.
E-mail address: hr681@uowmail.edu.au

1876-6102
Peer-review under responsibility of the scientific committee of the International Conference on Improving Residential Energy Efficiency.
10.1016/j.egypro.2017.08.008

energy efficient technologies have been investigated over the last two decades. The integration of phase change materials (PCMs) with photovoltaic thermal (PVT) collectors is attracting increasing attention, as PVT collectors can generate both electricity and thermal energy simultaneously, while the PCMs with high energy storage densities can be used as an effective solution to solve the mismatch between the thermal energy generation from the PVT collectors and building heating demand.

Nomenclature

A	area of each control volume along the PVT length (m^2)
c_p	specific heat (kJ/kg K)
G_t	total horizontal solar radiation (W/m^2)
h	enthalpy (kJ/kg)
h_c	forced convection coefficient (kg/h m^2 K)
h_{nc}	natural convection coefficient for stagnant air layer (kg/h m^2 K)
h_r	radiation heat transfer coefficient (kJ/h m^2 K)
h_w	wind convection coefficient (kJ/h m^2 K)
H_{fin}	fin height (m)
I_t	global solar insolation on the PVT surface (kJ/h m^2)
k	thermal conductivity (W/m K)
m	mass (kg)
$\dot{m}$	air mass flow rate (kg/h)
M	mass per unit area (kg/m^2)
$\dot{q}$	heat flux (W/m^2)
T	temperature (^oC)
v	velocity (m/s)
W	PVT width (m)

Greek symbols

δ	thickness (m)
ρ	density (kg/m^3)

Subscripts

amb	ambient air
b	bottom plate
f	flowing air
fin	longitudinal fin
g	glass cover
pv	photovoltaic plate
ref	reference

A number of studies have reported the integration of PCM thermal energy storage (TES) units with PVT collectors. For instance, Malvi *et al.* [2] numerically investigated a PVT system incorporating PCMs for dwelling application. The simulation results indicated that the PV output of the proposed system was increased by 9% with an average water temperature rise of 20°C in comparison with a PV-only system. Fiorentini *et al.* [3] presented a solar-assisted HVAC system in which the thermal energy generated by the PVT collector was stored in an air-based PCM TES unit and used to regulate the building heating demand. Lin *et al.* [4] developed a PCM-enhanced ceiling ventilation system integrated with air-based PVT collectors. The simulation results showed that this system can improve the indoor thermal comfort during winter time using the low-grade thermal heat generated from the PVT collectors. Lin *et al.* [5] also investigated the potential of using thermal energy generated by the PVT collectors for heating PCM-enhanced buildings. It was found that the PVT collectors could effectively improve the

indoor thermal performance of the house without using air conditioning systems in winter conditions, and the use of the PCM can greatly reduce the indoor temperature fluctuations. Al Imam *et al.* [6] examined the performance of a water-based PVT collector with a PCM layer under the absorber plate for thermal storage. The experimental results showed that the PVT thermal efficiency was in the range of 40-50% in winter, while that of the flat plate collectors without the PCM was around 35%.

This paper presents the performance evaluation of an integrated PVT-PCM TES system. A PCM model considering the hysteresis phenomenon during the phase change process was developed to simulate the thermal performance of the PCM TES unit. The thermal energy generated from the PVT collectors was temporarily stored in the PCM TES unit and then used later for space heating during winter. The thermal performance of the integrated PVT-PCM TES system was examined in terms of a performance indicator of the useful energy stored, based on a set of simulation trial tests designed using Taguchi method.

2. System modelling and methodology

2.1. System description and modelling

The integrated PVT-PCM TES system is illustrated in Fig. 1, in which the PVT collectors and a PCM TES unit are connected in series. During the daytime, the thermal energy generated from the PVT collectors can be stored in the PCM TES unit or can be directly used for space heating when there is a demand. During the night-time, the stored heat in the PCM TES unit can be used for space heating.

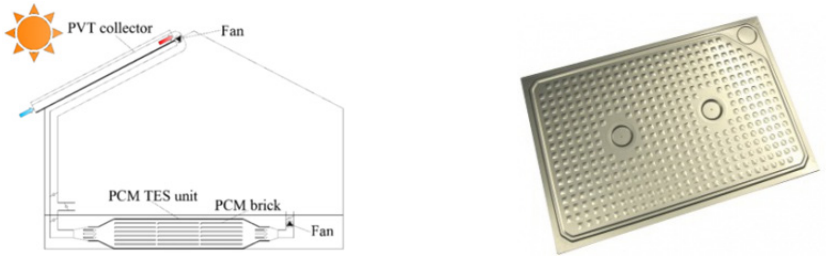

Fig. 1. (a) Schematic of the integrated PVT-PCM TES system and; (b) PCM brick considered in this study [7].

A PVT collector with fins and a glass cover [8] was used in this study, as shown in Fig. 2. The glass cover was placed above the PV plate, creating an air gap between the two plates as the thermal insulation. The PV plate was attached to an absorber plate through an adhesive layer. A number of air channels where the heat transfer fluid flows through were created between the absorber and the bottom plate of the PVT collector, and fins were used to enhance the convection heat transfer in the air channels. The bottom plate was insulated in order to reduce the heat transfer between the PVT collectors and the roof-top of the building.

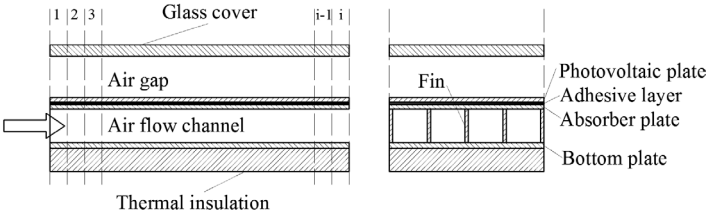

Fig. 2. Schematic of the PVT collector.

The performance of the PVT collector was simulated using a dynamic model developed in an earlier study [8], in which the PVT was first discretized into multiple control volumes along the air flow direction and further discretized vertically into six nodes including the glass cover, PV plate, absorber plate, fins, fluid air, and the bottom plate. The key governing equations of the glass cover and the fluid air are described in Eqs. (1) and (2),

respectively. The governing equations of the other nodes can be described in the same way. All the governing equations were solved with a Crank-Nicolson scheme. More details of this model can be found in [8].

$$Ac_{p,g}M_g\frac{\partial T_{g,i}}{\partial t} =$$
$$\alpha_g I_t A + h_{nc}A\left(T_{pv,i} - T_{g,i}\right) + h_{r,pv-g}A\left(T_{pv,i} - T_{g,i}\right) + h_w A\left(T_{amb} - T_{g,i}\right) + h_{r,g-sky}A\left(T_{sky} - T_{g,i}\right) \quad (1)$$

$$c_{p,f}\rho_f \Delta x\left(WH_{fin}\right)\frac{\partial T_{f,i}}{\partial t} + c_{p,f}\dot{m}_f \Delta x\frac{\partial T_{f,i}}{\partial x} =$$
$$h_{c,p-f}A\left(T_{p,i} - T_{f,i}\right) + h_{c,b-f}A\left(T_{b,i} - T_{f,i}\right) + 2h_{c,fin-f}A_{fin}\left(T_{fin,i} - T_{f,i}\right) \quad (2)$$

The PCM TES unit was simulated using a finite-difference model developed using an enthalpy method. The key assumptions used in the model development are as follows.

- The convection heat transfer within the liquid PCM was neglected and the conduction heat transfer within the PCM bricks was considered one-dimensional;
- The specific heat capacity of the liquid PCM and solid PCM beyond the phase change region was assumed to be identical and constant;
- The conduction heat transfer between the adjacent PCM bricks and the radiation heat transfer from the surfaces inside the TES unit were neglected;
- In each air channel, the air temperature variation only existed along the air flow direction;
- The air velocities in all air channels separated by the PCM layers were the same; and
- There was no natural convection of air within the TES unit.

The schematic of the nodes in the modelling of the PCM TES unit is presented in Fig. 3. A number of PCM arrays were arranged in parallel to form the PCM TES unit, in which the air channels were created between the PCM arrays. Each PCM layer consisted of multiple PCM bricks (see Fig. 1), based on which the PCM TES unit was divided into multiple sections containing both air nodes and PCM bricks, along with the air flow direction (see Fig. 3). The governing equations for the energy balance of each PCM node and each air node are expressed in Eqs. (3) and (4), respectively. The left-hand side term in Eq. (3) represents the energy storage rate in a single PCM node, while the right-hand side term represents the conductive heat transfer among the PCM nodes across the air flow direction. The boundary condition in Eq. (3) is the convection heat transfer to the air flowing through the air channels. The left-hand side term in Eq. (4) represents the energy storage rate of an air node, and the first right-hand side term represents the energy change rate of the air node along the air flow direction and the other one represents the convection heat gain from the PCM nodes above and beneath the air nodes.

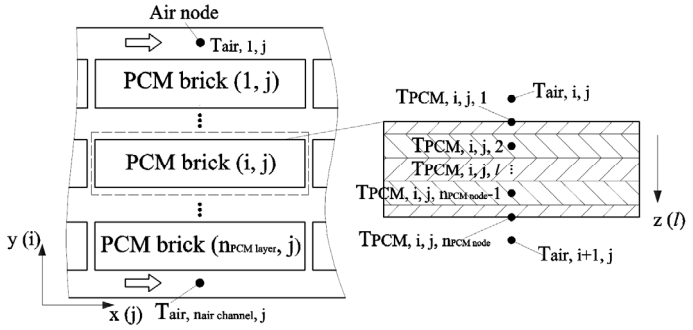

Fig. 3. Schematic of the nodes in the modelling of the PCM TES unit.

Gnielinski equation was used to calculate the heat transfer coefficient of the turbulent flow, and Nusselt number, which is a function of the ratio of the length to the width of air channels, was used to calculate the heat transfer coefficient of the laminar flow. The governing equations were solved based on the enthalpy-temperature relationship of the PCM, which can be obtained from the Differential Scanning Calorimetry (DSC) test or from the data sheets provided by manufacturers.

$$\begin{cases} \rho_{PCM}\frac{\partial h_{PCM}}{\partial t} = k_{PCM}\frac{\partial^2 T_{PCM}}{\partial y^2} \\ boundary\ conditions:\ k_{PCM}\frac{\partial T_{PCM}}{\partial y}\Big|_{l=1\ or\ n_{PCM\ node}} = \dot{q}_{convection} \end{cases} \quad (3)$$

$$\frac{\partial T_{air}}{\partial t} = v_{air}\frac{\partial T_{air}}{\partial x} + \frac{\dot{q}_{up}+\dot{q}_{down}}{\rho_{air}c_{p,air}\delta_{air}} \quad (4)$$

2.2. Performance indicator

A performance indicator, named as useful energy stored (UES), was developed and used to evaluate the amount of the useful thermal energy stored in the PCM TES unit, which was considered to be useful for space heating. It was defined as the useful thermal energy stored in the PCM based on a reference enthalpy, as expressed in Eq. (5). The reference enthalpy was assumed as the enthalpy of a PCM at 20°C.

$$\text{UES} = m(h - h_{ref}) \quad (5)$$

2.3. Simulation design using Taguchi method

In this study, Taguchi method was used to design trial simulations based on an orthogonal array in order to obtain the maximum amount of the information on the thermal performance of the system with a minimum number of simulation exercises. Analysis of variance (ANOVA) was used to investigate the response significance of the individual factors and identify the percentage contribution of each factor to the objective function. The sum of squares of factors, the pure sum of squares of factors, the variance of factors and percentage contribution of factors were the key statistic parameters used in ANOVA [9]. Five parameters, including the PCM type, the thickness of the PCM brick, the length of the PCM TES unit, the PCM charging air flow rate, and the size of the air gap between the glass cover and the PV cell in the PVT collector were selected as the control factors for performance analysis since these variables have been reported to be critical to the performance of PVT collectors and PCM TES units [10-12]. The PCMs considered in this study were SP24E and SP26E available from Rubitherm with a melting range of 24-25°C and 25-27°C, respectively [7]. Other control factors were designed to have three levels as summarised in Table 1. An L_{18} ($2^1\times3^7$) orthogonal array was used to design the simulation cases and the resulted orthogonal array is shown in Table 1.

Table 1. Control factors and their corresponding factor levels.

Factor level	Type of PCM	Thickness of the PCM brick (mm)	Length (m)	Air flow rate (kg/h)	Size of the air gap (mm)
1	SP24E	10	3.0	1000	5
2	SP26E	20	4.5	1500	12
3		30	6.0	2000	20

3. Results and discussions

3.1. Setup the tests

The thermal performance of the proposed system was evaluated under Melbourne winter weather conditions. The useful energy stored during the daytime was used as the objective response for performance evaluation.

The PVT collectors were assumed to be installed on a Solar Decathlon house [4] with an installation area of 4 m (L)×10 m (W). The configuration of the PCM TES unit used was similar to that of Charvát *et al*. [10]. The storage capacity of the TES unit was determined based on two days of the heating demand of the house [3] and therefore the same amount of the PCM was used when varying the thickness of the PCM brick and the length of the TES unit. The size of the air channels was determined based on the recommendations from Dolado *et al.* [11]. The number of the air channels was therefore determined based on the given thickness of the PCM brick and the length

of the TES unit. The specifications of the PVT collector and the PCM TES unit are summarised in Table 2. As the solar radiation may not be strong during the early morning and late afternoon in winter, it was assumed that the PCM TES unit was charged using the thermal energy collected by the PVT from 9:00 to 16:00. During this period, if the temperature of the outlet air from the PVT collectors was lower than the equivalent temperature of the PCM TES unit, the charging process will be suspended and it will be restarted once the outlet air temperature from the PVT collectors was high enough. The discharging process was assumed to be from 16.00 to 9:00 of next day. It is noted that the equivalent temperature of the PCM TES unit was obtained according to the average enthalpy of the PCM TES unit which was the average enthalpy of all PCM nodes in the TES unit. The inlet air temperature of the PCM TES unit during the discharging process was assumed as 20°C in this study by assuming that the return air from the indoor space can be used for thermal discharge. The simulations were carried out for three days and the results of the last day were presented to demonstrate the performance of the proposed integrated system. Fig. 4 shows the ambient air temperature and the total horizontal solar radiation (G_t) of the selected last day.

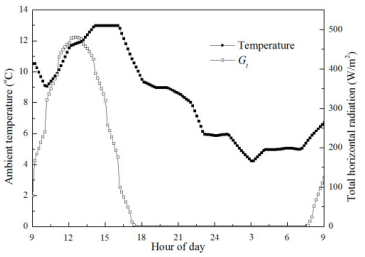

Fig. 4. Weather data used for performance evaluation.

Table 2. Specifications of the PVT collectors and the PCM TES unit.

PVT collector		PCM TES unit	
Total length (m)	4	Length (m)	3/4.5/6
Total width (m)	10	Width (m)	0.44
Slope (degree)	18.4	Dimension of PCM brick (mm)	Length: 450mm; width:300mm; thickness: 10/20/30
Number of fins	65	Size of the air channels (mm)	10
Size of the air gap (mm)	5/12/20	Rugosity of PCM brick (mm)	0.25
Air flow rate (kg/h)	1000/1500/2000	PCM type	SP24E/SP26E
		Number of PCM bricks	200

3.2. Results of model validation

To validate the model of the PCM TES unit developed, the experimental data reported by Lopez *et al.* [13] was used and the results are presented in Fig. 5. The model developed was modified in order to have the same configuration as that of the experimental setup used by Lopez *et al.* [13] through reducing the number of the air channels to two and assuming that the external surface of the TES unit was well-insulated. It can be seen that the simulated outlet air temperature from the PCM TES under both charging and discharging processes matched well with that of the experimental data, indicating that the model developed can provide an acceptable estimation.

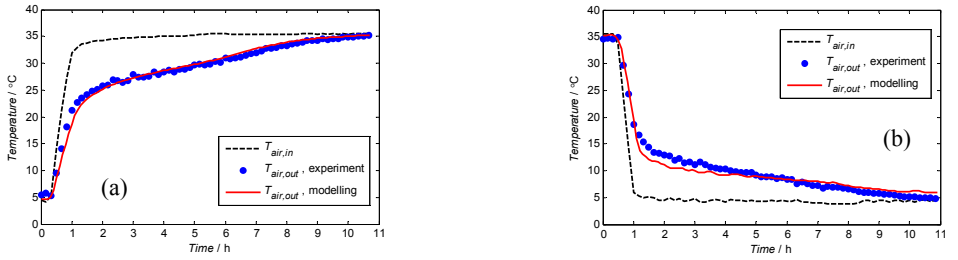

Fig. 5. Model validation (a) charging process, (b) discharging process.

3.3. Results of thermal performance evaluation

Table 3 summarises the Taguchi experiments and the corresponding results of each trial test. The results of ANOVA are presented in Table 4. It can be found that the air flow rate in the charging process was ranked as the most significant factor with a percentage contribution of 69.77% (Table 4), and the PCM type was the second significant factor (20.93%). The other factors such as the thickness of the PCM brick, the length of the PCM TES unit, and the size of the air gap were found insignificant, which indicated that the change of these three factors has a limited impact on the useful energy stored in the PCM TES unit under the test range studied.

Table 3. Results of the trial tests.

Test No.	Type of the PCM used	Thickness of the PCM brick (mm)	Length of the TES unit (m)	PCM charging air flow rate (kg/h)	Size of the air gap (mm)	Useful energy stored (kWh)
1	SP24E	10	3.0	1000	5	23.527
2	SP24E	10	4.5	1500	12	33.932
3	SP24E	10	6.0	2000	20	30.845
4	SP24E	20	3.0	1000	12	18.619
5	SP24E	20	4.5	1500	20	33.890
6	SP24E	20	6.0	2000	5	27.047
7	SP24E	30	3.0	1500	5	31.466
8	SP24E	30	4.5	2000	12	31.436
9	SP24E	30	6.0	1000	20	19.467
10	SP26E	10	3.0	2000	20	22.246
11	SP26E	10	4.5	1000	5	13.625
12	SP26E	10	6.0	1500	12	29.645
13	SP26E	20	3.0	1500	20	27.456
14	SP26E	20	4.5	2000	5	21.583
15	SP26E	20	6.0	1000	12	17.113
16	SP26E	30	3.0	2000	12	23.956
17	SP26E	30	4.5	1000	20	16.926
18	SP26E	30	6.0	1500	5	26.988

Table 4. Analysis of variance table.

Control factors	Degree of freedom	Sum of squares	Variance	Variance ratio	Pure sum of squares	Percentage contribution
Type of the PCM used	1	142.759	142.759	34.891	138.667	20.93%
Thickness of PCM brick	2	5.509	2.754	0.673	-2.674	-0.40%
Length of the TES unit	2	1.765	0.883	0.216	-6.418	-0.97%
PCM charging air flow rate	2	470.498	235.249	57.496	462.315	69.77%
Size of the air gap	2	9.332	4.666	1.140	1.148	0.17%
All other/error	8	32.733	4.092	1.000	69.557	10.50%
Total	17	662.595	38.976			100.00%

From Table 3, it can be observed that a higher useful energy stored in the TES system (i.e. higher than 30 kWh) was obtained in the trial tests 2, 3, 5, 7, and 8 when the PCM SP24E was used, and a higher useful energy stored in the TES system was also achieved when the charging air flow rate was 1500 kg/h (i.e. trial tests 2, 5, and 7). From the above results, it seems that the PCM type of SP24E and the air flow rate of 1500 kg/h were the best levels considered in this study.

Among all trial simulations, the highest useful energy stored in the TES system was achieved under the test condition specified in the trail test 2. The inlet and outlet air temperatures of the PCM TES unit, the equivalent temperature of the PCM TES unit, and the accumulated useful energy stored in this test case are presented in Fig. 6. It can be observed that the charging process started at around 10:00 and stopped at around 14:10 in the test day as the outlet air temperature of the PVT collectors (i.e. the inlet air temperature of the TES unit) was lower than the equivalent temperature of the PCM TES unit from 9:00 to 10:00 and from 14:10 to 16:00. It is noted that the inlet and outlet air temperatures of the PCM TES unit during the time periods of 9:00-10:00 and 14:10-16:00 were not illustrated as there was no thermal energy was charged into the TES unit. During the discharge process, the outlet air temperature and the equivalent temperature of the PCM TES unit first dropped rapidly due to the sensible heat release and then dropped very slowly due to the phase change of the PCM. In this test day, the outlet air

temperature of the PCM TES unit remained at least 2.0°C higher than the inlet air temperature of 20°C during the whole discharge process.

The above results showed that the performance of the TES unit is highly influenced by the key design variables and these key design variables should be selected carefully in order to satisfy the specific requirements of a particular application such as the storage capacity and the heat charging/discharging rate.

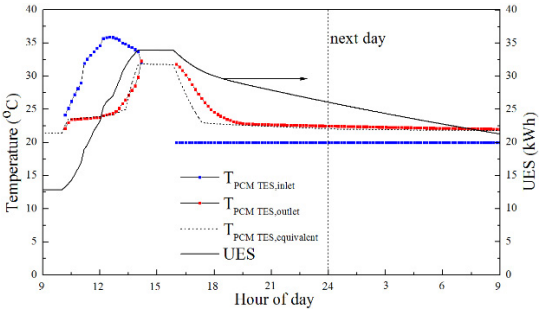

Fig. 6. Results of the trial test 2.

4. Conclusions

This paper investigated the performance evaluation of an integrated PVT-PCM TES system using Taguchi method. A performance indicator, named as the useful energy stored in the PCM TES unit, was used as the objective response for Taguchi experiments. Five factors, including the PCM type, the thickness of the PCM brick in the TES unit, the length of the PCM TES unit, the PCM charge air flow rate, and the size of the air gap between the glass cover and the PV cell of the PVT collector, were considered as the control factors. The results showed that the PCM type and the PCM charging air flow rate are the significant factors that influence the useful energy stored in the PCM TES unit. Among the test ranges defined and the PCM types considered, the PCM SP24E and the charging air flow rate of 1500kg/h could provide a better indoor thermal performance in terms of the useful energy stored. The results from this study can be used to facilitate the design of the PVT-PCM integrated systems.

References

[1] U.S. Energy Information Administration, http://www.eia.gov/consumption/ (accessed 26.10.2016).
[2] Malvi CS, Dixon-Hardy DW, Crook R. Energy balance model of combined photovoltaic solar-thermal system incorporating phase change material. Solar Energy. 2011;85(7):1440-6.
[3] Fiorentini M, Cooper P, Ma Z. Development and optimization of an innovative HVAC system with integrated PVT and PCM thermal storage for a net-zero energy retrofitted house. Energy and Buildings. 2015;94:21-32.
[4] Lin W, Ma Z, Sohel MI, Cooper P. Development and evaluation of a ceiling ventilation system enhanced by solar photovoltaic thermal collectors and phase change materials. Energy conversion and management. 2014;88:218-30.
[5] Lin W, Ma Z, Cooper P, Sohel MI, Yang L. Thermal performance investigation and optimization of buildings with integrated phase change materials and solar photovoltaic thermal collectors. Energy and Buildings. 2016;116:562-73.
[6] Al Imam MF, Beg RA, Rahman MS, Khan MZ. Performance of PVT solar collector with compound parabolic concentrator and phase change materials. Energy and Buildings. 2016;113:139-44.
[7] Rubitherma PCMs, www.rubitherm.com (accessed 26.10.2016).
[8] Fan W, Kokogiannakis G, Ma Z, Cooper P. Development of a dynamic model for a hybrid photovoltaic thermal collector–Solar air heater with fins. Renewable Energy. 2017;101:816-34.
[9] Roy RK. A primer on the Taguchi method. 2nd ed. Michigan: Society of Manufacturing Engineers; 2010.
[10] Charvát P, Klimeš L, Ostrý M. Numerical and experimental investigation of a PCM-based thermal storage unit for solar air systems. Energy and Buildings. 2014 ;68:488-97.
[11] Dolado P, Lazaro A, Marin JM, Zalba B. Characterization of melting and solidification in a real scale PCM-air heat exchanger: Numerical model and experimental validation. Energy Conversion and Management. 2011;52(4):1890-907.
[12] Duffie JA, Beckman WA. Solar engineering of thermal processes. 4th ed. New York: Wiley; 2013.
[13] Lopez JP, Kuznik F, Baillis D, Virgone J. Numerical modeling and experimental validation of a PCM to air heat exchanger. Energy and Buildings. 2013;64:415-22.